Frontiers of Physics
https://doi.org/10.1007/s11467-021-1113-6
Front. Phys.
17(2), 22503 (2022)

RESEARCH ARTICLE

Experimental investigation of light storage of diffraction-free and quasi-diffraction-free beams in hot atomic gas cell

Chengyuan Wang[1], Yun Chen[1], Zibin Jiang[1], Ya Yu[1], Mingtao Cao[2,†], Dong Wei[1], Hong Gao[1,‡], Fuli Li[1]

[1] *Ministry of Education Key Laboratory for Nonequilibrium Synthesis and Modulation of Condensed Matter, Shaanxi Province Key Laboratory of Quantum Information and Quantum Optoelectronic Devices, School of Physics, Xi'an Jiaotong University, Xi'an 710049, China*
[2] *Key Laboratory of Time and Frequency Primary Standards, National Time Service Center, Chinese Academy of Sciences, Xi'an 710600, China*
Corresponding authors. E-mail: [†] *caomingtao1987@163.com,* [‡] *honggao@mail.xjtu.edu.cn*
Received April 25, 2021; accepted August 24, 2021

In this article we report on the experimental investigation of light storage for several types of diffraction-free beams (Bessel and Airy beams) and quasi-diffraction-free beams by utilizing electromagnetically induced transparency (EIT) technique in a hot atomic gas cell. The experimental results show that the diffraction-free and quasi-diffraction-free beams have better storage performances when compared with ordinary images possessing similar spatial profiles. Meanwhile, the Bessel beams and the quasi-diffraction-free images are able to maintain their spatial profiles with a long storage time while the side-lobes of the Airy beam are gradually depleted with the increment of the storage time. We quantitatively analyze the storage results and give physical explanations behind these phenomena. Furthermore, the self-healing of the retrieved diffraction-free beams is verified, signifying that their characteristics preserve well after storage.

Keywords quantum memory, electromagnetically induced transparency, diffraction-free beam

1 Introduction

Optical storage occupies an important role in quantum information processing [1, 2] and has been extensively explored in recent decades [3, 4]. A variety of schemes, such as electromagnetically induced transparency (EIT) [5, 6], Autler–Townes splitting (ATS) [7], Raman absorption [8], and gradient echo memory (GEM) [9], have been proposed to realize light storage with different figure of merits. Among these schemes, EIT storage is the most prevalent candidate due to its lenient experimental conditions and high storage efficiency [10–14]. Much progress has been achieved for EIT storage, especially in the media of hot alkali atomic vapor. For instance, Novikova *et al.* realized 45% storage efficiency in a hot Rb vapor by using the pulse-shape optimization method [10]. Katz *et al.* prolonged the storage time to one second by mapping the light field onto spin orientation within a decoherence-free subspace of spin states [12]. Besides, it is also possible to store quantum states such as arbitrary polarization states [15, 16] and orbital angular momentum (OAM) states [17].

Nowadays, lots of research interests have been focused on the storage of two-dimensional (2D) wave packets since they have the potential to increase the spatial multimode capacity in quantum information [18–21]. Diffraction-free beams like Airy beams and Bessel beams are representative 2D wave packets that can preserve their spatial profiles during propagation in free space and even in the turbulent or scattering environment [22], which benefits them to be excellent candidates in optical communication. In contrast, normal 2D wave packets are more vulnerable to environmental turbulence. To overcome this, several schemes were proposed to modulate an arbitrary wave packet's angular spectrum into a shape similar to that of the Bessel beam. This new kind of beam, called quasi-diffraction-free beam, is also able to propagate a long distance while maintaining its transverse intensity distribution [23, 24]. Up to now, those studies mainly focus on the generation and propagation dynamics of the diffraction-free and quasi-diffraction-free beams [25, 26], while realizing the optical storage of such beams can expand their applications in optical communication and quantum communication. Hang *et al.* theoretically proposed that an Airy temporal profile combined with a spatial Bessel or

* This article can also be found at http://journal.hep.com.cn/fop/EN/10.1007/s11467-021-1113-6.

Airy beam can withstand both diffraction and dispersion in a linear propagation regime [27]. Wang *et al.* successfully stored the Airy wave packet in a solid-state medium and checked the property of the retrieved Airy wave packet by monitoring its self-healing ability during the propagation [21]. Recently, Smartsev *et al.* studied the coherent diffusion of group-velocity slowed Bessel–Gaussian fields with EIT assisted four-wave mixing scheme [28]. When stored in atomic media, the light field is totally transferred into atomic ground state coherence. In media such as crystals and cold atomic ensembles, the atoms are stationary or motionless; while in the hot atomic gas cell, atoms exhibit dramatically thermal motion. Hence after a certain storage time, the atoms' positions redistribute, which disturbs the structure of the stored wave packet [29, 30]. Whether the family of diffraction-free and quasi-diffraction-free beams could withstand the atomic motion-induced diffusion and survive after being stored in the hot atomic gas cell is an interesting and open question worth exploring.

In this article, we experimentally investigate the EIT storage of diffraction-free beams and quasi-diffraction-free images in a hot atomic gas cell. The outcomes show that Bessel beams and quasi-diffraction-free images have higher storage fidelities than Airy beams. Besides, all of them show better storage performance than light fields with similar intensity profiles. In the end, the self-healing abilities of the retrieved diffraction-free beams are further verified, manifesting that their properties keep well after storage.

2 Experimental results and discussion

The schematic experimental setup is illustrated in Fig. 1(a). A 5 cm long ^{87}Rb atomic gas cell containing 8 torr neon buffer gas is placed inside a three-layer μ-metal magnetic shielding oven and kept at 60°C. The horizontally polarized probe beam with 10 μW power and 2 mm diameter is modulated from a Gaussian profile to the diffraction-free and quasi-diffraction-free beams via a computer-controlled liquid crystal spatial light modulator (SLM, Hamamatsu, x10468). Then the shaped probe beam is imaged to the center of the atomic cell by a 4f system and further captured by an intensified charge-coupled device (ICCD, istar 334T) through another 4f system. The vertically polarized control beam, with 15 mW power and 4 mm diameter, propagates collinearly with the probe beam through the first polarizing beam splitter (PBS1). After passing through the atomic cell, they are separated by PBS2.

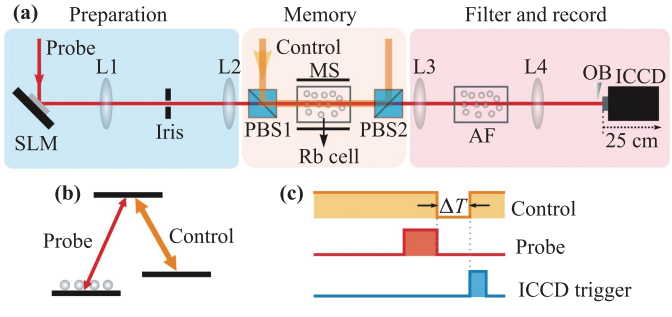

Fig. 1 **(a)** Schematic of the experimental setup, **(b)** energy level, and **(c)** time sequence for EIT storage in a hot ^{87}Rb atomic gas cell. (SLM, spatial light modulator; PBS, polarizing beam splitter; L1, L2, L3 and L4, lenses with the same focal length of $f = 500$ mm; MS, μ-metal magnetic shielding; AF, atomic filter; OB, opaque blockage; ICCD, intensified charge-coupled device.)

The energy level structure is shown in Fig. 1(b). The 795 nm probe laser is frequency-locked at D1 line with $|5S_{1/2}, F = 1\rangle \rightarrow |5P_{1/2}, F' = 1\rangle$ transition. The control laser is phase-locked to the probe laser with the aid of an offset phase lock servo (OPLS, D2-135) and is on-resonant to $|5S_{1/2}, F = 2\rangle \rightarrow |5P_{1/2}, F' = 1\rangle$ transition. These two light fields form a typical Λ-type EIT system to perform the light storage experiment. At the noise filter stage, we choose the typical solution of an atomic filter (AF), which is an 80°C rubidium cell with most of the atoms populated in $|5S_{1/2}, F = 2\rangle$, to further absorb the residual control beam leaked from PBS2.

The corresponding time sequence is shown in Fig. 1(c). The control beam is turned on in advance to prepare most of the atoms into $|5S_{1/2}, F = 1\rangle$, then it is adiabatically turned off at the time when the 2 μs probe pulse enters into the atomic medium. Consequently, the probe beam is absorbed and transferred into atomic collective spin excitation. After a certain storage time (ΔT), the control beam is switched on again to release the stored probe beam. The ICCD is activated synchronously with the reopened control beam by a trigger signal to record the retrieved beam. In order to obtain images with a high signal-to-noise ratio (SNR), the gating switch is opened for 500 ns to segregate the scattering noises existed throughout the whole experiment window.

Firstly we investigate the storage of a 2D Airy wave packet, which can be expressed as

$$\psi_{Airy}(x, y) = Ai\,(x/x_0)\exp\,(ax/x_0) \cdot Ai\,(y/y_0)\exp\,(ay/y_0)\,, \quad (1)$$

where $Ai\,(x/x_0)$ and $Ai\,(y/y_0)$ represent the Airy function, and a is the exponential truncation factor. The 2D Airy probe beam (ψ_{Airy}) before storage is presented in Fig. 2(a1), while Figs. 2(a2)–(a4) show the retrieved signals with ΔT setting at 0.4 μs, 0.8 μs, and 1.2 μs, respectively. For comparison, we also store an ordinary image ($|\psi_{Airy}|$, the module of ψ_{Airy}) whose profile is similar to the Airy beam, but with a constant phase front, see Fig. 2(b1). The corresponding storage results are shown in Figs. 2(b2)–(b4). The outcomes demonstrate that ψ_{Airy} is able to maintain its spatial profile while $|\psi_{Airy}|$ becomes

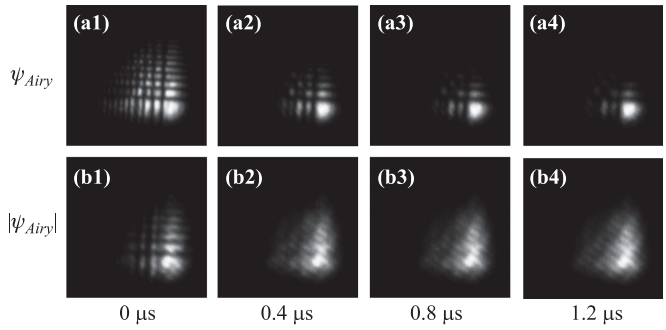

Fig. 2 Optical storage of Airy beam (ψ_{Airy}) and its analogue ($|\psi_{Airy}|$) in the atomic vapor cell. **(a1)** and **(b1)** are patterns of ψ_{Airy} and $|\psi_{Airy}|$ before storage (0 μs), while (a2–a4) and (b2–b4) correspond to the retrieved patterns with the storage time of 0.4 μs, 0.8 μs, and 1.2 μs, respectively.

too blurred to be recognised under the same storage time. It should also be noted that the side-lobes of ψ_{Airy} are gradually depleted with the increment of storage time.

Next we attempt to store Bessel beams, which are able to be extended to high dimensions and increase information capacity in optical communication [31]. The nth order Bessel beam is written as

$$\psi_n(\boldsymbol{r}) = a_n J_n(k_r r) \exp\left[\mathrm{i}\left(k_z z + n\phi\right)\right], \tag{2}$$

where $\boldsymbol{r} = (r, \phi)$ denotes the polar coordinate, a_n is the complex coefficient, J_n is the Bessel function, k_r and k_z are the transverse and longitudinal wave numbers respectively. In this experiment, Bessel beams with first-order (ψ_0) and second-order (ψ_2) are stored for proof of principle. For comparision, an ordinary image ($|\psi_2|$) that only retains the intensity distribution of ψ_2 is stored under the same circumstances. The experimental results are exhibited in Figs. 3(a1)–(a4), (b1)–(b4), and (c1)–(c4) for ψ_0, ψ_2, and $|\psi_2|$ with different storage durations. It can be observed that the shapes of the retrived Bessel beams keep well up to 6 μs storage time while $|\psi_2|$ suffers severe dispersion.

For quantitatively comparing the results above, we take out the horizontal cross section at the main-lob and the adjacent dark region of ψ_{Airy} and $|\psi_{Airy}|$ in Fig. 2, and calculate the fringe visibility of each image. In Fig. 3, the horizontal cross-section at the center area of each Bessel image is also extracted for the visibility calculation. The results are shown in Figs. 4(a) and (b). By comparing the results in Fig. 2, Fig. 3, and Fig. 4, we can conclude that ψ_{Airy} and $\psi_{0(2)}$ maintain higher visibilities than $|\psi_{Airy}|$ and $|\psi_2|$ after storage. Meanwhile, the Bessel beams are capable of keeping their overall shape unchanged with 6 μs storage time while the Airy beam loses many details only with 1.2 μs storage time.

Theoretically, the evolution of a light field $\psi(\boldsymbol{r}, t)$ under atomic diffusion can be deduced by solving the diffusion

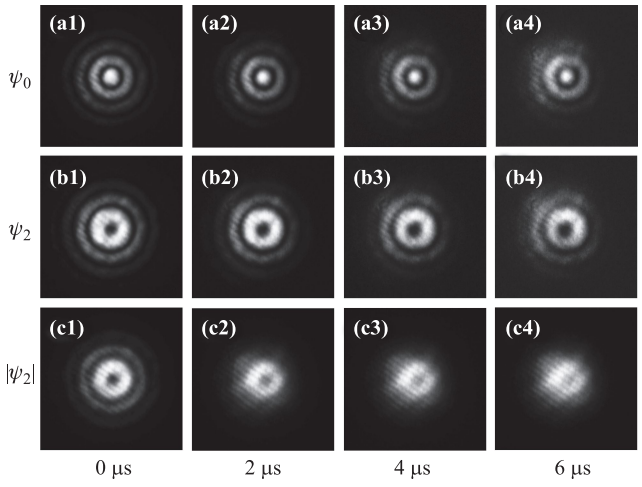

Fig. 3 Storing the first order Bessel beam (ψ_0), the second order Bessel beam (ψ_2) and its analogue ($|\psi_2|$). **(a1–a4)**, **(b1–b4)**, and **(c1–c4)** correspond to storing ψ_0, ψ_2, and $|\psi_2|$ with storage time of 0 μs, 2 μs, 4 μs, and 6 μs, respectively.

equation [32, 33]:

$$\frac{\partial}{\partial t}\psi(\boldsymbol{r}, t) = D\nabla_r^2 \psi(\boldsymbol{r}, t), \tag{3}$$

where D is the diffusion coefficient and t is the diffusion time. By Fourier transforming to the wave-vector space $\tilde{\psi}(\boldsymbol{k}) = \int \frac{\mathrm{d}^2\boldsymbol{r}}{2\pi}\psi(\boldsymbol{r})\mathrm{e}^{-\mathrm{i}\boldsymbol{k}\cdot\boldsymbol{r}}$, we can obtain the solution of Eq. (3) as $\tilde{\psi}(\boldsymbol{k}, t) = \tilde{\psi}(\boldsymbol{k}, 0)\mathrm{e}^{-D|\boldsymbol{k}|^2 t}$. This implies that if a light field has a broad spatial frequency ($|\boldsymbol{k}|^2$) distribution in Fourier space, the higher spatial frequency component will undergo more severe attenuation than the lower. As a result, its outline is distorted tremendously and eventually becomes unrecognizable. On the contrary, if a light field has a narrow spatial frequency distribution, the attenuation of each spatial frequency component will be identical, thus the influence of atomic diffusion would be slender.

For the Airy beam, the spatial frequency of the main lob is much smaller than that of the side lobs. Hence the side lobs deplete much faster with the increment of the storage time, as can be seen in Figs. 2(a1)–(a4). However, the image contrast between each lob preserves very well, even with the storage time up to 1.2 μs. By compari-

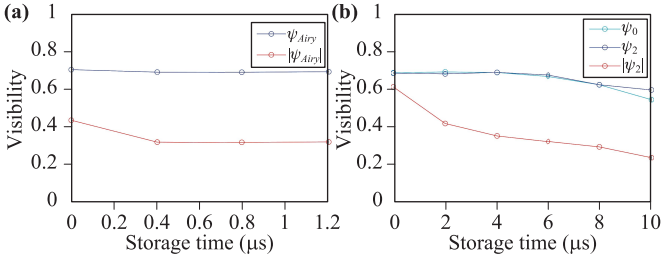

Fig. 4 The fringe visibility of each image in Fig. 2 and Fig. 3 as a function of storage time.

son, the image contrast of $|\psi_{Airy}|$ drops severely at 0.4 μs. The physics behind this phenomenon is that the adjacent lobs of ψ_{Airy} have π phase difference, which introduces destructive interference when transferring the ground-state coherence to the light field [32].

On the other hand, the Fourier transform of a Bessel beam is the so-called perfect vortex beam [34], which is a thin ring and possesses a very narrow spatial frequency distribution [35]. So it will add a unique attenuation term and the overall spatial structure of the beam keeps invariant after diffusion, as can be seen in Fig. 3 for the cases of ψ_0 and ψ_2. In contrast, $|\psi_2|$ has multiple frequency components and is more subtle to atomic diffusion.

In a word, when storing a 2D wave packet, e.g., an arbitrary image, in the hot atomic gas cell, its spatial frequency distribution is the most critical factor affecting the storage results. However, most of the 2D images have very broad and complicated spatial frequency distributions, which are susceptible to atomic diffusion and have poor storage performance. Even though lots of schemes, such as the phase-shift lithography technique [32], storing Fraunhofer diffraction pattern of an image [19], and the correlation-imaging technique [20], are capable of improving the resolutions of the retrieved images, their high-frequency components are still inevitably dispersed, resulting in the loss of the image information. Seeking a more efficient method is anticipated. The above results give us an inspiration that if we can engineer the angular spectrum of an image to constrain its spatial frequency over a thin ring, just as the Bessel beam, its storage time and storage fidelity could be remarkably improved. Recently, several schemes have been proposed to modulate the spatial frequency of an arbitrary image into a narrow ring in order to suppress its diffraction during propagation [23, 24]. But the angular spectrum ring width produced in this way cannot be infinitesimal as that of the ideal Bessel beams, so this kind of beam is named quasi-diffraction-free beam. So far, there is still no report on modulating arbitrary images as quasi-diffraction-free beams to prompt their storage properties. Here we also investigate the storage performance of several quasi-diffraction-free images (marked as I_{q1}, I_{q2}, and I_{q3} in Fig. 5). These quasi-diffraction-free images are generated with the method in Ref. [23] and all of their angular spectra are modulated into thin rings (insets in Fig. 5). As can be observed from Figs. 5(a2)–(a4), (c2)–(c4), and (d2)–(d4) that the profiles of these images maintain well up to 6 μs storage duration, manifesting that the quasi-diffraction-free beams are also robust to atomic diffusion. For comparison, we also store a normal image with broad spatial frequency distribution ($|I_{q1}|$), whose profile becomes unrecognizable in less than 2 μs. This method can help to retain the image's overall spatial structure to the greatest extent and has ascendancy over the previous schemes [19, 20, 32]. For more complicated images, one can adopt the method such as [36] to modulate them into quasi-diffraction-free beams, but their intensity profiles are not exactly the same as the original ones. Besides, it is worth mention that the thin ring distributed angular spectrum is not a requisite condition to resist the diffusion influence. For instance, the elegant optical modes [37], such as elegant Hermite–Gaussian beams and elegant Laguerre–Gaussian beams can also resist diffusion, but their angular spectra are not thin rings and they are not propagation invariant.

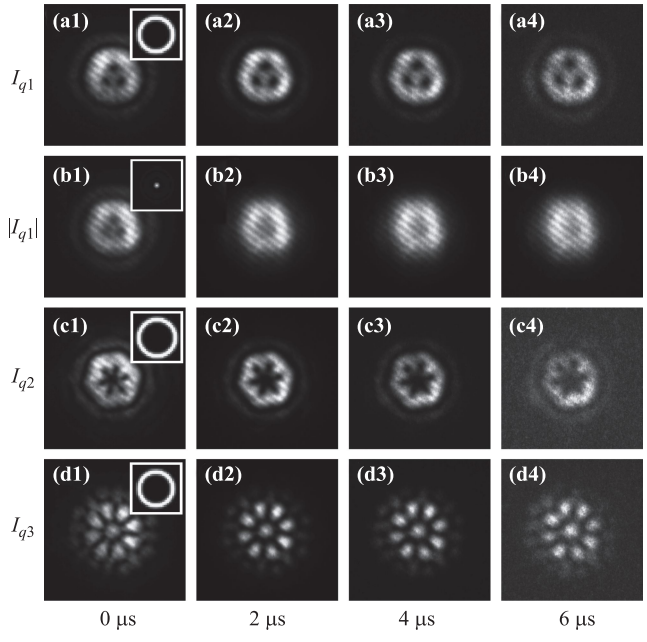

Fig. 5 Storing several quasi-diffraction-free images (I_{q1}, I_{q2}, and I_{q3}) with spatial frequencies distributed over a thin ring and a normal image ($|I_{q1}|$) with broad spatial frequency distribution. The insets are their corresponding angular spectra.

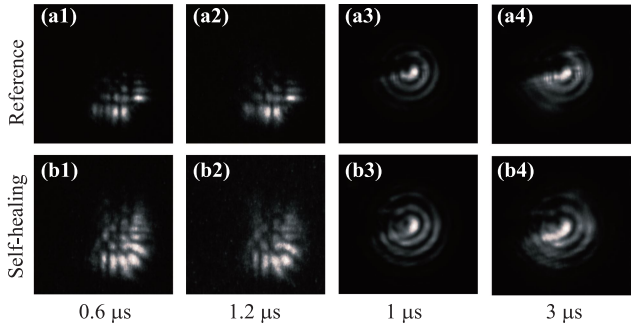

Fig. 6 The self-healing results of the retrieved Airy beam (ψ_{Airy}) and the first-order Bessel beam (ψ_1). **(a1–a2)** correspond to the profiles of ψ_{Airy} with the storage time of 0.6 μs and 1.2 μs, while **(a3–a4)** correspond to ψ_1 with the storage time of 1 μs and 3 μs when parts of their bodies are blocked. **(b1–b2)** and **(b3–b4)** correspond to the profiles of reconstructed ψ_{Airy} and ψ_1 when the ICCD is translated backward by a distance of 25 cm.

Self-healing is a striking property of the diffraction-free beams, which has been extensively investigated in recent years [22, 38, 39]. Here we further evaluate the characteristics of the retrieved diffraction-free beams by verifying their self-healing abilities. In particular, for the Airy beam, parts of its side-lobes are depleted after the storage process. It has not been explored whether the Airy beam is able to be self-reconstructed under this circumstance. As shown in Fig. 1(a), an opaque blockage (OB) is placed at the focal plane of L4 to obstruct the main-lobs of the retrieved Airy beams, whose profiles are given in Figs. 6(a1) and (a2) with the storage time of 0.6 μs and 1.2 μs, respectively. Next the ICCD is translated backward by a distance of 25 cm and records the evolved probe beams, as shown in Figs. 6(b1) and (b2). It can be clearly seen that the main lobs are regenerated after various storage durations, indicating that the self-healing property of the Airy beam remains even suffering from atomic diffusion. We also take the first order (ψ_1) Bessel beam to study its self-healing property. An opaque conical object is placed at the focal plane of L4 to block partial areas of the retrieved Bessel beam on the left side. The profiles of the blocked Bessel beams are shown in Figs. 6(a3) and (a4) with the storage time of 1 μs and 3 μs. Figures 6(b3) and (b4) present their corresponding reformations after propagating a distance of 25 cm. The results show that the blocked parts are almost reborn in both circumstances, which further proves that the diffraction-free beams can maintain their properties well after the storage process.

3 Conclusion

To conclude, we experimentally investigate the optical storage of diffraction-free beams and quasi-diffraction-free images based on the on-resonant Λ-type EIT storage scheme in a hot atomic gas cell. The experimental results show that both the Airy and the Bessel beams have better storage performances when compared to the ordinary images with similar spatial profiles. Meanwhile, the Bessel beams are able to maintain their spatial profiles while the side-lobes of the Airy beam are gradually depleted with the increment of the storage time. We further demonstrate that when an arbitrary 2D image is modulated into a quasi-diffraction-free beam, its storage performance could also be improved dramatically. In addition, the self-healing abilities of the retrieved beams further indicate that the diffraction-free beams can retain their characteristics well after storage. Our research results have guiding significances in high fidelity storage of spatial multi-modes, manipulation of diffraction-free beams, and high-dimensional quantum communication.

Acknowledgements This work was supported by the National Natural Science Foundation of China (NSFC) (Grant Nos. 11774286, 92050103, 12104358, 11534008, 12033007, and 61875205).

References

1. L. M. Duan, M. D. Lukin, J. I. Cirac, and P. Zoller, Long-distance quantum communication with atomic ensembles and linear optics, *Nature* 414(6862), 413 (2001)
2. H. J. Kimble, The quantum internet, *Nature* 453(7198), 1023 (2008)
3. A. I. Lvovsky, B. C. Sanders, and W. Tittel, Optical quantum memory, *Nat. Photonics* 3(12), 706 (2009)
4. K. Heshami, D. G. England, P. C. Humphreys, P. J. Bustard, V. M. Acosta, J. Nunn, and B. J. Sussman, Quantum memories: Emerging applications and recent advances, *J. Mod. Opt.* 63(20), 2005 (2016)
5. I. Novikova, R. L. Walsworth, and Y. Xiao, Electromagnetically induced transparency-based slow and stored light in warm atoms, *Laser Photon. Rev.* 6(3), 333 (2012)
6. T. Jeong and H. S. Moon, Improvement of light storage efficiency using targetable optical pumping, *Opt. Commun.* 427, 596 (2018)
7. E. Saglamyurek, T. Hrushevskyi, A. Rastogi, K. Heshami, and L. J. Leblanc, Coherent storage and manipulation of broadband photons via dynamically controlled Autler–Townes splitting, *Nat. Photonics* 12(12), 774 (2018)
8. J. Guo, X. Feng, P. Yang, Z. Yu, L. Q. Chen, C. Yuan, and W. Zhang, High performance raman quantum memory with optimal control in room temperature atoms, *Nat. Commun.* 10(1), 148 (2019)
9. Q. Glorieux, J. B. Clark, A. M. Marino, Z. Zhou, and P. D. Lett, Temporally multiplexed storage of images in a gradient echo memory, *Opt. Express* 20(11), 12350 (2012)
10. I. Novikova, A. V. Gorshkov, D. F. Phillips, A. S. Sørensen, M. D. Lukin, and R. L. Walsworth, Optimal control of light pulse storage and retrieval, *Phys. Rev. Lett.* 98(24), 243602 (2007)
11. Y. H. Chen, M. J. Lee, I. C. Wang, S. Du, Y. F. Chen, Y. C. Chen, and I. A. Yu, Coherent optical memory with high storage efficiency and large fractional delay, *Phys. Rev. Lett.* 110(8), 083601 (2013)
12. O. Katz and O. Firstenberg, Light storage for one second in room-temperature alkali vapor, *Nat. Commun.* 9(1), 2074 (2018)
13. Y. Wang, J. Li, S. Zhang, K. Su, Y. Zhou, K. Liao, S. Du, H. Yan, and S. L. Zhu, Efficient quantum memory for single-photon polarization qubits, *Nat. Photonics* 13(5), 346 (2019)
14. C. Wang, Y. Yu, Y. Chen, M. Cao, J. Wang, X. Yang, S. Qiu, D. Wei, H. Gao, and F. Li, Efficient quantum memory of orbital angular momentum qubits in cold atoms, *Quantum Sci. Technol.* 6(4), 045008 (2021)
15. Y. W. Cho and Y. H. Kim, Atomic vapor quantum memory for a photonic polarization qubit, *Opt. Express* 18(25), 25786 (2010)
16. Y. H. Ye, M. X. Dong, Y. C. Yu, D. S. Ding, and B. S. Shi, Experimental realization of optical storage of vector beams of light in warm atomic vapor, *Opt. Lett.* 44(7), 1528 (2019)

17. S. Shi, D. S. Ding, W. Zhang, Z. Y. Zhou, M. X. Dong, S. L. Liu, K. Wang, B. S. Shi, and G. C. Guo, Transverse azimuthal dephasing of a vortex spin wave in a hot atomic gas, *Phys. Rev. A* 95(3), 033823 (2017)
18. Y. W. Cho and Y. H. Kim, Storage and retrieval of thermal light in warm atomic vapor, *Phys. Rev. A* 82(3), 033830 (2010)
19. P. K. Vudyasetu, R. M. Camacho, and J. C. Howell, Storage and retrieval of multimode transverse images in hot atomic rubidium vapor, *Phys. Rev. Lett.* 100(12), 123903 (2008)
20. Y. W. Cho, J. Oh, and Y. H. Kim, Diffusion-free image storage in hot atomic vapor, *Phys. Rev. A* 86(1), 013844 (2012)
21. L. Wang, Y. Sun, R. Wang, X. Zhang, Y. Chen, Z. Kang, H. Wang, and J. Gao, Storage of airy wavepackets based on electromagnetically induced transparency, *Opt. Express* 27(5), 6370 (2019)
22. J. Broky, G. A. Siviloglou, A. Dogariu, and D. N. Christodoulides, Self-healing properties of optical airy beams, *Opt. Express* 16(17), 12880 (2008)
23. C. López-Mariscal and K. Helmerson, Shaped nondiffracting beams, *Opt. Lett.* 35(8), 1215 (2010)
24. A. F. Martínez-Herrera, A. Céspedes-Mota, and S. Lopez-Aguayo, Divide and conquer algorithm for nondiffracting beams, *J. Opt. Soc. Am. A* 36(12), 1968 (2019)
25. M. Mazilu, D. J. Stevenson, F. Gunn-Moore, and K. Dholakia, Light beats the spread: "non-diffracting" beams, *Laser Photonics Rev.* 4(4), 529 (2010)
26. Z. K. Wu, H. Guo, W. Wang, and Y. Z. Gu, Evolution of finite energy airy beams in cubic-quintic atomic vapor system, *Front. Phys.* 13(1), 134201 (2018)
27. C. Hang, Z. Bai, and G. Huang, Storage and retrieval of airy light wave packets in a coherent atomic system, *Phys. Rev. A* 90(2), 023822 (2014)
28. S. Smartsev, R. Chriki, D. Eger, O. Firstenberg, and N. Davidson, Structured beams invariant to coherent diffusion, *Opt. Express* 28(22), 33708 (2020)
29. R. Pugatch, M. Shuker, O. Firstenberg, A. Ron, and N. Davidson, Topological stability of stored optical vortices, *Phys. Rev. Lett.* 98(20), 203601 (2007)
30. O. Firstenberg, M. Shuker, A. Ron, and N. Davidson, Coherent diffusion of polaritons in atomic media, *Rev. Mod. Phys.* 85(3), 941 (2013)
31. N. Ahmed, Z. Zhao, L. Li, H. Huang, M. P. J. Lavery, P. Liao, Y. Yan, Z. Wang, G. Xie, Y. Ren, A. Almaiman, A. J. Willner, S. Ashrafi, A. F. Molisch, M. Tur, and A. E. Willner, Mode-division multiplexing of multiple Bessel-Gaussian beams carrying orbital-angular-momentum for obstruction-tolerant freespace optical and millimetre-wave communication links, *Sci. Rep.* 6(1), 22082 (2016)
32. M. Shuker, O. Firstenberg, R. Pugatch, A. Ron, and N. Davidson, Storing images in warm atomic vapor, *Phys. Rev. Lett.* 100(22), 223601 (2008)
33. R. Chriki, S. Smartsev, D. Eger, O. Firstenberg, and N. Davidson, Coherent diffusion of partial spatial coherence, *Optica* 6(11), 1406 (2019)
34. J. Pinnell, V. Rodríguez-Fajardo, and A. Forbes, How perfect are perfect vortex beams? *Opt. Lett.* 44(22), 5614 (2019)
35. A. S. Ostrovsky, C. Rickenstorff-Parrao, and V. Arrizón, Generation of the "perfect" optical vortex using a liquid-crystal spatial light modulator, *Opt. Lett.* 38(4), 534 (2013)
36. A. Zannotti, C. Denz, M. A. Alonso, and M. R. Dennis, Shaping caustics into propagation-invariant light, *Nat. Commun.* 11(1), 3597 (2020)
37. O. Firstenberg, P. London, D. Yankelev, R. Pugatch, M. Shuker, and N. Davidson, Self-similar modes of coherent diffusion, *Phys. Rev. Lett.* 105(18), 183602 (2010)
38. S. Vyas, Y. Kozawa, and S. Sato, Self-healing of tightly focused scalar and vector Bessel–Gauss beams at the focal plane, *J. Opt. Soc. Am. A* 28(5), 837 (2011)
39. G. Milione, A. Dudley, T. A. Nguyen, O. Chakraborty, E. Karimi, A. Forbes, and R. R. Alfano, Measuring the self-healing of the spatially inhomogeneous states of polarization of vector Bessel beams, *J. Opt.* 17(3), 035617 (2015)